Supplemental material for "Gravitational wave detection with optical lattice atomic clocks"

S. Kolkowitz, I. Pikovski, N. Langellier, M.D. Lukin, R.L. Walsworth, J. Ye
(Dated: October 18, 2016)

I. DERIVATION OF THE EFFECTIVE DOPPLER SHIFT INDUCED BY A PASSING GRAVITATIONAL WAVE

A passing gravitational wave (GW) induces periodic changes in the light travel time between emitter and detector[1]. In this section we derive the magnitude of this effect as a function of the GW amplitude, the orientation between the satellites and the direction of propagation of the GW, and the distance between the clocks. Similar analyses have been performed for proposed detectors that utilize Doppler tracking [1] and pulsar timing [2]. Our detection scheme involves only a one-way link as in the case of pulsar timing, but with full experimental control on both sites for the emission and detection of the signal.

Weak gravitational fields are captured by a perturbed metric $g_{\mu\nu} = \eta_{\mu\nu} + h_{\mu\nu}$, where $\eta_{\mu\nu}$ is the Minkowski metric and $|h_{\mu\nu}| \ll 1$ is a small perturbation. GWs are described in the transverse traceless gauge by the metric:

$$g_{\mu\nu} = \begin{pmatrix} -1 & 0 & 0 & 0 \\ 0 & 1+h_+ & h_\times & 0 \\ 0 & h_\times & 1-h_+ & 0 \\ 0 & 0 & 0 & 1 \end{pmatrix}, \tag{S1}$$

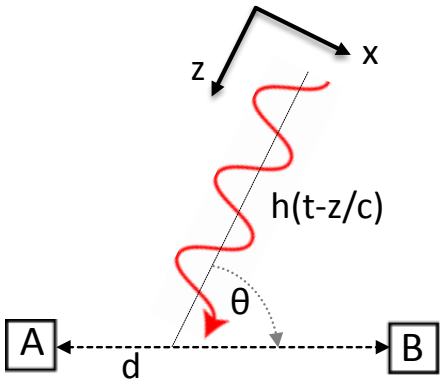

FIG. S1. A GW incident along the z-axis periodically changes the light travel distance between A and B.

[1] One can expect an additional effect due to the time dilation induced by the GW itself. However, this effect would be of second order in GW strain amplitude h, and is therefore vanishingly small when compared to the sensitivity of current clocks.

where $h_+(t-z/c)$ and $h_\times(t-z/c)$ correspond to the two polarizations of the wave, which travels in the z-direction. For simplicity we first calculate the effect for a plus-polarized plane wave with $h = h_+ = |h|e^{-i2\pi f(t-z/c)}$, where f is the frequency of the wave and $|h|$ its amplitude (arbitrary polarizations are restored with the substitution $|h| \to |h_+|\cos(2\psi) + |h_\times|\sin(2\psi)$, where ψ is the polarization angle). The line element for this metric is then

$$ds^2 = -c^2dt^2 + (1+h)dx^2 + (1-h)dy^2 + dz^2. \tag{S2}$$

We now consider the situation depicted in Fig. S1, where a light signal is sent at time t from system A to system B, which is at a distance d in the $x-z$-plane. A light-like curve is defined by $ds^2 = 0$. Parameterizing the curve by r with $x = r\sin\theta$, $y = 0$ and $z = r\cos\theta$, the coordinates for the curve become (to lowest order in h):

$$cdt = \left(1 + \frac{1}{2}h\sin^2\theta\right)dr. \tag{S3}$$

As the signal is emitted at coordinate time t and travels from A to B in a time $t_1 = t + d/c$ to lowest order in h, it travels an apparent distance

$$D_{AB} = c\int_t^{t_1} dt' = \int_0^d \left(1 + \frac{1}{2}h(1-\cos^2\theta)\right)dr, \tag{S4}$$

where the GW is parameterized by $h = h(t + r/c - r\cos\theta/c)$. In terms of the indefinite integral of the wave, H(t), the above expression becomes

$$D_{AB} = c(t_1 - t) = d + \frac{c}{2}(1+\cos\theta)\left[H(t) - H\left(t + \frac{d}{c}(1-\cos\theta)\right)\right]. \tag{S5}$$

In flat space the distance traveled by the light would just be given by d, but the presence of the GW periodically changes the apparent length of the light path. In Doppler tracking techniques, the signal is reflected back to A and measured there. Here, instead, we consider measurement directly on B. The rate of change gives a Doppler shift of the signal $\sigma \equiv \dot{D}_{AB}/c = \Delta\nu/\nu$, where ν is the optical frequency:

$$s = \frac{\Delta\nu}{\nu} = \frac{1+\cos\theta}{2}\left[h(t) - h\left(t + \frac{d}{c}(1-\cos\theta)\right)\right]. \tag{S6}$$

This apparent Doppler shift is the signal to be detected at B. The effect is maximized for $\theta = \pi/2$, i.e. for the

detector aligned perpendicularly to the GW, while the signal disappears for $\theta = 0$, i.e. in the direction of propagation of the GW. Similarly to interferometric detection schemes, the frequency shift is due to transversal motion of test bodies as the GW is passing.

From equation (S6), we can see that when using a single shared local oscillator to compare two clocks positioned a distance d apart in the plane ($\theta = \pi/2$) of a passing GW of amplitude $|h|$ and wavelength $\lambda_{\mathrm{GW}} = c/f$, the clocks will appear to "tick" at different rates, with the maximum fractional frequency difference between the two clocks given by

$$s_{max} = |h| \left| \sin\left(\pi \frac{d}{\lambda_{\mathrm{GW}}}\right) \right|. \tag{S7}$$

Note that the detector is insensitive to GWs with wavelengths that match a multiple of the baseline d.

II. DETECTOR SENSITIVITY

For space-based detectors, the effect of geometric factors on the sensitivity is typically described by the transfer function $\mathcal{T}(f)$, which captures the detector response to specific GW frequencies [3]. We can express Eq. (S6) in Fourier-space, which gives

$$\tilde{s}(f) = \frac{1}{2}\tilde{h}(f)\left(1 - e^{i2\pi f d/c}\right), \tag{S8}$$

where the tilde denotes the Fourier transform $\tilde{s}(f) = \int dt e^{i2\pi f t} s(t)$. The expression multiplying $\tilde{h}$ in Eq. (S8) depends only on the geometry of the detector and gives rise to its geometric transfer function, which is $\mathcal{T}_\nu(f) = |(1 - e^{i2\pi f d/c})/2|^2 = \sin^2(\pi f d/c)$. It is different than for the case of phase detectors in two ways: we consider only a single one-way link between two satellites, and are sensitive to frequency, i.e. changes in the phase of the light. For detectors sensitive to phase, the additional derivative results in the transfer function $\mathcal{T}_\phi(f) = \mathrm{sinc}^2(\pi f d/c)$ [4]. A comparison between the transfer functions of a phase and a frequency detector for an otherwise identical geometry is shown in Fig. S2.

The actual measured signal for the clock-based detector depends on the measurement scheme used for the atoms. A long integration time T increases the sensitivity (see Eq. 2 in the main text), but is limited by the atomic linewidth. The signal acquired for a clock measurement between t_0 and $t_0 + T$ is therefore

$$\bar{s} = \frac{1}{T}\left|\int_{t_0}^{T+t_0} dt s(t)\right| = \left|\int_{-\infty}^{\infty} dt F(t_0 - t) s(t)\right|, \tag{S9}$$

where $F(t)$ is a window function that captures the measurement sequence of duration T. For a Ramsey measurement (ignoring the finite pulse durations), the window function is just $F(t) = 1/T$ for $t \in [-T, 0]$ and $F(t) = 0$ otherwise. For a continuous GW with $h(t) = |h|\sin(2\pi f t + \varphi)$, this gives

$$\begin{aligned}\bar{s} = \frac{|h|}{\pi f T}\Bigg|&\sin\left(\pi f \frac{d}{c}\right)\sin(\pi f T) \times \\ &\times \cos\left(\pi f\left(2t_0 + \frac{d}{c} + T\right) + \varphi\right)\Bigg|.\end{aligned} \tag{S10}$$

As we consider a continuous signal, we can adapt the starting time of the measurement to account for φ and thus set the argument of the cosine to 0 to give

$$\bar{s} = |h|\left|\sin\left(\pi f \frac{d}{c}\right)\mathrm{sinc}(\pi f T)\right|. \tag{S11}$$

The sine term in Eq. (S11) captures the light-travel time between the two satellites, while the sinc-function appears due to intergation for a time T. Equivalently, we can describe the measurement by a transfer function $\mathcal{T}_T(f) = \mathcal{T}_\nu(f)\mathrm{sinc}^2(\pi f T)$, as can also be seen by using directly the Fourier transform of eq. (S9). Ideal sensitivity is achieved only for the frequency $f = 1/(2T)$ and distance $d = cT$. For higher frequency GWs, the signal strength is reduced due to the finite integration time T. Reducing the integration time to $T' < T$ gives an ideal signal at $2fT' = 1$, but causes the atomic clocks to be less sensitive due to atom projection noise.

Using dynamical decoupling allows the detector to be ideally sensitive at frequencies other than $1/(2T)$. Instead of the integrated signal given in Eq. (S9), the detection is performed with a window function $F_{dd}(t)$, such that

$$\bar{s}_{dd} = \left|\int_{-\infty}^{\infty} dt s(t) F_{dd}(t_0 - t)\right|. \tag{S12}$$

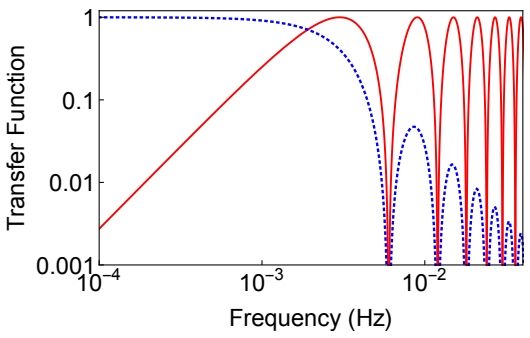

FIG. S2. Transfer functions for a detector sensitive to changes in frequency, $\mathcal{T}_\nu(f)$ (red curve), as compared to a detector sensitive to phase, $\mathcal{T}_\phi(f)$ (blue dotted curve). Frequency measurements yield the maximal signal for $f = (n + 1/2)c/d$, $n \in \mathbb{N}_0$, while the sensitivity is drastically reduced for $f < c/(2d)$. In contrast, phase measurements become significantly less sensitive for frequencies $f \gtrsim c/(2d)$, even without the presence of noise. Here the distance between satellites is $d = 5 \times 10^{10}$ m, as in the main text.

The window function is defined by the particular dynamical decoupling sequence that is utilized. For our purposes, we use the PDD sequence with n π-pulses, given by $TF_{dd}(-t) = \Theta(t) + 2\sum_{k=1}^{n}(-1)^k\Theta(t - kT/n) + (-1)^{n+1}\Theta(t - T)$, where $\Theta(x)$ is the Heaviside step function. Adapting the measurement time such that $\varphi + \pi f d/c = \pi/2$, the signal becomes

$$\bar{s}_{dd} = |h| \left| \sin\left(\pi f \frac{d}{c}\right) \operatorname{sinc}\left(\pi f \frac{T}{n}\right) \times \right. \\ \left. \times \frac{1}{n}\sum_{k=1}^{n}(-1)^{k+1} \sin\left(\pi f(2k-1)\frac{T}{n}\right) \right|. \tag{S13}$$

With DD, the signal is maximized for $f = n/(2T)$, but is reduced for other frequencies. Thus DD is ideal to select a specific frequency at which the detector is maximally sensitive. The minima closest to the main peak occur at $f = (n \pm 1)/(2T)$, we thus define the detector bandwidth as $\Delta f \approx 1/T$. Outside this frequency range the detector can still operate, but with a reduced sensitivity.

Restoring the angular dependence as in Eq. (S6), and averaging over all angles and polarizations, we get

$$\bar{s}_{dd} = |\langle h \rangle| \left| \sqrt{\frac{2}{3} - \frac{1}{(2\pi f \frac{d}{c})^2} + \frac{\sin(4\pi f \frac{d}{c})}{2(2\pi f \frac{d}{c})^3}} \operatorname{sinc}\left(\pi f \frac{T}{n}\right) \times \right. \\ \left. \times \frac{1}{n}\sum_{k=1}^{n}(-1)^{k+1} \sin\left(\pi f(2k-1)\frac{T}{n}\right) \right|, \tag{S14}$$

where $\langle h \rangle = \sqrt{|h_\times|^2 + |h_+|^2}/\sqrt{2}$ is the mean GW amplitude.

III. DERIVATION OF OPTICAL POWER REQUIREMENTS

Our proposed detector utilizes a phase-locked loop (PLL) to lock laser B in satellite B to the light sent from laser A in satellite A, such that the two lasers function as a single ultra-stable clock laser shared between the two satellites. Such a setup allows for correlated noise spectroscopy [5–7], which enables the Ramsey interrogation time T to be extended far beyond the laser coherence time (1 s) out to the atomic radiative lifetime (160 s). While laser frequency noise arising from the laser linewidth Δ_L can be eliminated using this technique, shot noise on the optical link and the finite bandwidth of the PLL will give rise to relative phase noise between Laser A and B. Here we analyze the power requirements stemming from the individual laser linewidths, dead time between measurements, Rabi frequency, and the shot noise in the PLL. Because of the differential measurement, our system can then be viewed as a single clock probed by a laser with noise given by the fractional relative frequency between Laser A and B, $y = \delta\nu/\nu$, and we denote the uncertainty in the relative frequency as

$$\sigma_y^2 = \langle \bar{\delta\nu}^2 \rangle / \nu^2, \tag{S15}$$

where $\bar{\delta\nu} = (1/\tau)\int_{t_0}^{t_0+\tau} \delta\nu(t)dt$ is the average relative frequency in a measurement window of time τ. The above expression is the true variance of the average frequency, in practice the Allan variance (or two-sample variance) is a more practical measure of the frequency instability [8]. We can express the integral again as a convolution with a window function $h(t)$, which captures the sensitivity to frequency noise during a measurement of duration τ: $\sigma_y^2 = \langle \left(\int_{-\infty}^{\infty} dt h(t_0 - t) y(t) \right)^2 \rangle$, or in Fourier space

$$\sigma_y^2 = \int_0^\infty df |\tilde{H}(f)|^2 S_y(f), \tag{S16}$$

where we expressed the variance in terms of the one-sided power spectral density (PSD) $S_y(f)$ and the noise transfer function of the measurement, given by the Fourier transform $\tilde{H}(f) = \int dt e^{i2\pi f t} h(t)$. The window function $h(t)$ is determined by the applied spectroscopy sequence, including the Rabi frequency and pattern of the applied atomic control pulses, the dead time between subsequent sequences, and the number of averaged measurements. In contrast, the noise spectrum $S_y(f)$ is completely independent of the measurement protocol, and is instead determined by the design of the PLL, the individual laser linewidths, and the optical power received at satellite B.

We first consider $S_y(f)$, using a simple model which captures the main features of a PLL (for a detailed analysis of phase-locked loops and various loop designs, see Refs. [9, 10]). We assume that the laser phase ϕ^B is updated in a time step t_k according to $\phi^B_{k+1} = \phi^B_k + \phi^{corr}_k$, where ϕ^{corr}_k is an applied correction based on the outcome of the heterodyne measurement of lasers A and B. The demodulated outcome is a signal $i \propto \sin(\phi^A - \phi^B)$ with a shot noise contribution n. For small phase differences $\delta\phi = \phi^A - \phi^B$ and a loop bandwidth B, the correction in the loop is $\phi^{corr}_k = B\int_{t_k}^{t_k+1/B} \delta\phi_k + n(t_k)$. Without shot noise, this loop would give $\phi^B_{k+1} \to \phi^A_k$ in the limit of arbitrarily large bandwidth. However, the shot noise restricts the bandwidth, as it increases with larger B. For times $t \gg 1/B$, we can treat the steps as infinitesimal and obtain a loop differential equation $\dot{\delta\phi} = -B\delta\phi - \nu + Bn(t)$, where ν is the laser frequency. Writing this in Fourier space, we obtain the noise power spectral density

$$S_\varphi(f) = \frac{\Delta_L}{(2\pi f)^2 + B^2} + \frac{h\nu B^2}{\eta P_B((2\pi f)^2 + B^2)}, \tag{S17}$$

where B is the loop bandwidth, Δ_L is the linewidth of the two lasers, P_B is the received power from satellite A at the PLL photodetector, and η is the detection efficiency. The first term is due to white frequency noise from the two laser linewidths, which is suppressed in the PLL within the bandwidth B, while the second term is

the photon shot noise of the optical link, which sets the noise floor for the heterodyne detection in the PLL.The bandwidth of the loop can be optimized to minimize the additional phase noise, which gives the optimal bandwidth $B_{opt} = \sqrt{\eta P_B \Delta_L/(h\nu)}$.

The noise transfer function $|\tilde{H}(f)|^2$ in Eq. (S16) depends on the precise details of the spectroscopy sequence. For the sake of brevity and clarity we restrict our present analysis to Ramsey measurements. We note that for spectroscopic sequences other than Ramsey, additional susceptibility to photon shot noise can be introduced [11]. DD operation may therefore require additional optical power than Ramsey, and will be studied in detail in future works. The sensitivity function $h(t)$ describes the response of the atoms to frequency fluctuations [12], and for Ramsey interrogation it is given by $h(t) = 1$ during the free precession period of length T, and $h(t) = \sin(\Omega_R t)$ ($h(t) = -\sin(\Omega_R t)$) during the first (second) $\pi/2$ pulse, where Ω_R is the Rabi frequency. The total measurement consists of n repetitions of Ramsey interrogations. Each interrogation cycle is of duration $T_c = T + T_D + 2t_p$, where T_D is the dead time, $r = T/T_c$ is the duty cycle, t_p the pulse duration and $\tau = nT_c$ is the total measurement time. For $\pi/2$ pulses, $t_p = \pi/(2\Omega_R)$, the noise transfer function is then

$$|\tilde{H}(f)|^2 = \frac{1}{n^2T^2}\frac{\Omega_R^2}{((2\pi f)^2-\Omega_R^2)^2}\left(\frac{\Omega_R}{\pi f}\sin(\pi f T) + 2\cos\left(\pi f T + \pi^2\frac{f}{\Omega_R}\right)\right)^2 \frac{\sin^2(\pi f n T_c)}{\sin^2(\pi f T_c)}. \quad \text{(S18)}$$

Here, the last term captures the finite dead time in-between measurements, which can significantly alter the scaling of the noise with averaging time. We therefore consider two cases, that of zero dead time ($T_D = 0$), and that of finite dead time ($T_D > 0$). The transfer functions for three representative cases are plotted in Fig. 3.

If there is no dead time and for $\Omega_R \gg B$, the noise transfer function in Eq. S18 simplifies dramatically to become $|\tilde{H}(f)|^2 = \mathrm{sinc}^2(\pi f T)$ and the integral can be computed analytically to give $\int_0^\infty df \sin^2(\pi f\tau)/((2\pi f)^2 + B^2) = (1-e^{-B\tau})/(8B)$. Including the atom projection noise given in the main text, the overall variance in frequency measurement for $r = 1$ is therefore

$$\sigma^2 = \frac{1}{(2\pi\nu)^2 T\tau}\left(\frac{1}{N} + \frac{1-e^{-B\tau}}{2\tau/T}\left(\frac{\Delta_L}{B} + \frac{h\nu}{\eta P_B}B\right)\right). \quad \text{(S19)}$$

For optimized loop bandwidth B_{opt} and in the limit $B\tau \gg 1$, the above expression becomes

$$\sigma^2 = \frac{1}{(2\pi\nu)^2 T\tau}\left(\frac{1}{N} + \frac{T}{\tau}\sqrt{\frac{h\nu\Delta_L}{\eta P_B}}\right). \quad \text{(S20)}$$

In this limit, the contribution from laser phase noise averages down as $\sigma_L^2 \propto 1/\tau^2$, consistent with other Doppler tracking detectors [13]. As a result, the photon shot noise averages down faster than the atom projection noise, and at long averaging times atom projection noise will dominate (see Fig. S4).

Zero dead time clock operation has been realized using interleaved measurements of two clocks [14, 15]. However, if our detector is restricted to only a single clock per satellite, detector operation will likely include a small but finite time between subsequent measurements, which introduces additional noise through a process known as the Dick effect [16]. For the clock GW detector, the dead time results in aliasing down of the high frequency noise in the PLL, resulting in differential frequency noise in the two-clock comparison, which can limit the differential clock stability. We emphasize that this differential Dick noise is distinct from the aliased laser frequency noise traditionally referred to as Dick noise. While "traditional" Dick noise will also be present in each individual clock making up the detector, it is common mode and will be cancelled out in the synchronous comparison. In order to account for the differential Dick noise due to finite dead time ($T_D > 0$), integration over the full transfer function has to be performed. This was done using numeric integration for a finite number of measurements n, and analytically for the limit $n \to \infty$.

Any finite dead time will alias the high frequency differential laser noise in the PLL into differential white frequency noise, resulting in a Dick noise term which scales as $\sigma_D^2 \propto 1/\tau$. Because this term averages down more slowly than the $\sigma_L^2 \propto 1/\tau^2$ term in Eq. (S20), at some finite number of measurements, n_D, σ_D will begin to dominate over σ_L. Numerical integration of Eq. (S16), with Eqs. (S17) and (S18) for finite n, and in the limits $\Omega_R \gg B_{opt}$, $T_D \gg 1/\Omega_R$, and $T \gg T_D$, yields $\sigma_D^2 \approx (n/n_D) \times \sigma_L^2$, where $n_D \approx 1/(2\pi T_D B_{opt})$. Therefore, for n sequential measurements the differential Dick noise can be safely ignored for small enough dead

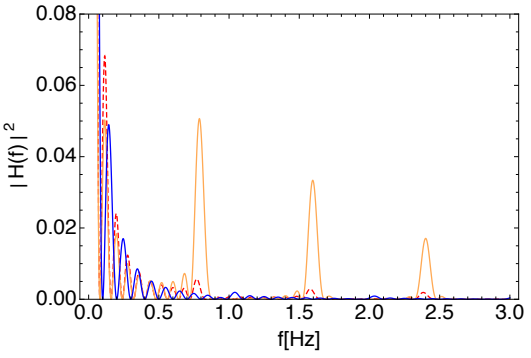

FIG. S3. Transfer function capturing the sensitivity to frequency fluctuations, eq. (S18). The blue dashed curve shows the case for $n = 10$ measurements with no dead time and $\Omega_R = 100$ Hz. The orange and red curves show the transfer functions for $n = 10$, and $r = 0.8$, with $\Omega_R = 100$ Hz (orange curve) and $\Omega_R = 10$ Hz (red dashed curve), and the Ramsey time $T = 1$ s. Spikes appear due to the Dick effect at frequencies $f = r/T$. The transfer function attenuates frequencies above Ω_R and thus acts as an effective low-pass filter.

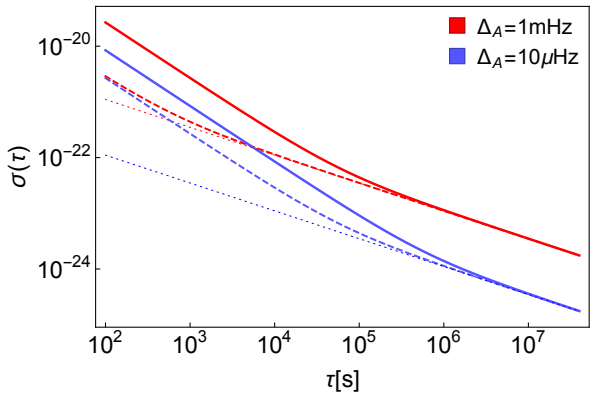

FIG. S4. Fractional frequency instability as a function of averaging time τ as given in Eq. (S20), for the case of zero dead time ($r = 1$). The red curves correspond to an atomic linewidth $\Delta_A = 1$ mHz as in the main text, while the blue curves are for a narrower atomic transition with $\Delta_A = 10\mu$Hz. The thick and dashed lines differ by the received optical power: 95 pW (red thick line), 10 nW (blue thick line) and 1μW (blue and red dashed lines). The dotted lines show the atom projection noise limit as given in Eq. 2 of the main text. For short averaging times photon shot noise dominates and the noise scales with $1/\tau$, while at long averaging times atom projection noise dominates and the noise scales as $1/\sqrt{\tau}$.

times, with the condition $nT_D \ll 1/(B_{opt})$, while in the limit of many measurements, the Dick noise will always dominate.

For current individual optical lattice clocks $T_D \approx 1$ s, and $T_D \gg 1/B_{opt}$. In this case, and in the limit of many measurements, the full integral in Eq. (S16) with Eqs. (S17) and (S18) can be evaluated analytically using the property of the Fejér-kernel: $F(x) = \sin^2(nx)/(\sin^2(x)n) \to \pi\delta(x)$ on $x \in [-\pi/2, \pi/2]$. The resulting frequency uncertainty from laser noise becomes

$$\sigma_L^2 = \frac{8\Omega_R^2 B}{(2\pi\nu)^2\tau T^2}\sum_{k=0}^{\infty}\frac{\frac{\Delta_L}{B}+\frac{h\nu}{\eta P_B}B}{\left(2\pi\frac{kr}{T}\right)^2+B^2}\frac{1}{\left(\left(2\pi\frac{kr}{T}\right)^2-\Omega_R^2\right)^2} \times\left(\Omega_R\sin(\pi kr)+2\pi\frac{kr}{T}\cos(\pi kr+2\pi t_p kr/T)\right)^2. \tag{S21}$$

The contribution from laser phase noise now averages down more slowly, $\sigma_L^2 \propto 1/\tau$, thereby competing directly with atom projection noise. However, the Rabi frequency Ω_R used in the Ramsey sequence can be used as a lowpass filter on the atomic response in order to limit the susceptibility to high frequency noise resulting from the Dick effect, as shown in Fig. S3. As long as the PLL bandwidth B_{opt} is kept above Ω_R, the PLL can bridge the dead time between subsequent Ramsey sequences, suppressing the differential laser noise, and the noise spectrum experienced by the atoms is simply the photon shot noise from the PLL detection during the Ramsey control pulses. For $\Omega_R \ll B_{opt}$, Eq. S21 then simplifies to (now again including atom projection noise)

$$\sigma^2 = \frac{1}{(2\pi\nu)^2 T\tau}\left(\frac{1}{N}+\frac{2}{r}\frac{h\nu}{\eta P_B}\Omega_R\right) \tag{S22}$$

This corresponds to the intuitive condition that the number of photons received at satellite B during the Ramsey control pulses must be larger than the number of atoms N used in each run of the measurement.

IV. TIME CONSTRAINTS FOR NARROWBAND SIGNAL OBSERVATION

The narrowband nature of the clock detector means that averaging and observation time will be fundamentally limited by the duration of the GW at the specific frequency of interest. Compact binary inspirals produce continuous GWs which experience a chirp towards higher frequencies, given by [17]:

$$\dot{f} = \frac{96}{5}\pi\left(\frac{\pi G M_c}{c^3}\right)^{5/3} f^{11/3}, \tag{S23}$$

where G is the gravitational constant and $M_c = (m_1 m_2)^{3/5}/(m_1+m_2)^{1/5}$ is the effective chirp mass of a binary system with masses m_1 and m_2. The number of GW cycles in a time $t \in [t_1, t_2]$ small compared to the GW period is $dn_{cyc} = f dt$, or $n_{cyc} = \int_{f_1}^{f_2} df f/\dot{f}$. Assuming $f_2 - f_1 \approx 1/T_{max}$, we find that the time the GW is within this frequency range is given by

$$\tau_{\rm GW} = \frac{n_{cyc}}{f} \approx 2.5\times 10^{10}{\rm s}\left(\frac{10{\rm mHz}}{f}\right)^{8/3}\left(\frac{2.6M_\odot}{M_c}\right)^{5/3}, \tag{S24}$$

where $M_\odot = 2\times 10^{30}$ kg is the solar mass, and we have normalized M_c to the mass value for an inspiral of two objects with $m_1 = m_2 = 3M_\odot$. For such sources, and for frequencies in the ∼10 mHz range, the GW has an essentially fixed frequency over hundreds of years. For heavier sources, however, $\tau_{\rm GW}$ can be much shorter; for a black hole binary as detected by LIGO ($m_1 = 36M_\odot, m_2 = 29M_\odot$) we have $\tau_{\rm GW} \approx 15$ years in the above frequency range around $f = 10$ mHz. For optimal GW detection, we require $\tau_{av} < \tau_{\rm GW}$, which is reasonable for most sources expected in the frequency range of interest. We also note that this is not a strict limitation for a source with a known frequency chirp, as the measurement sequence can be easily adapted to chirp the detection window along with the source.

[1] F. B. Estabrook and H. D. Wahlquist, General Relativity and Gravitation **6**, 439 (1975).
[2] S. Detweiler, The Astrophysical Journal **234**, 1100 (1979).
[3] N. J. Cornish and L. J. Rubbo, Physical Review D **67**, 022001 (2003).
[4] R. Schilling, Classical and Quantum Gravity **14**, 1513 (1997).
[5] C. W. Chou, D. B. Hume, J. C. J. Koelemeij, D. J. Wineland, and T. Rosenband, Phys. Rev. Lett. **104**, 070802 (2010).
[6] M. Takamoto, T. Takano, and H. Katori, Nature Photonics **5**, 288 (2011).
[7] T. Nicholson, M. Martin, J. Williams, B. Bloom, M. Bishof, M. Swallows, S. Campbell, and J. Ye, Phys. Rev. Lett. **109**, 230801 (2012).
[8] J. Rutman, Proceedings of the IEEE **66**, 1048 (1978).
[9] L. G. Kazovsky, J. Lightwave Technol. **4**, 182 (1986).
[10] C. C. Chen and C. S. Gardner, NASA STI/Recon Technical Report N **87** (1987).
[11] Z. Chen, J. G. Bohnet, J. M. Weiner, and J. K. Thompson, Physical Review A **86**, 032313 (2012).
[12] G. Santarelli, C. Audoin, A. Makdissi, P. Laurent, G. J. Dick, and A. Clairon, IEEE transactions on ultrasonics, ferroelectrics, and frequency control **45**, 887 (1998).
[13] J. W. Armstrong, Living Rev. Relativity **9**, E2 (2006).
[14] G. Biedermann, K. Takase, X. Wu, L. Deslauriers, S. Roy, and M. Kasevich, Physical review letters **111**, 170802 (2013).
[15] M. Schioppo, R. Brown, W. McGrew, N. Hinkley, R. Fasano, K. Beloy, T. Yoon, G. Milani, D. Nicolodi, J. Sherman, *et al.*, arXiv preprint arXiv:1607.06867 (2016).
[16] L. L. Presti, D. Rovera, and A. De Marchi, IEEE transactions on ultrasonics, ferroelectrics, and frequency control **45**, 899 (1998).
[17] M. Maggiore, *Gravitational waves* (Oxford Univ. Press, 2008).